A COUPLED-FIELD ANALYSIS ON A 500 MHz SUPERCONDUCTING RADIO FREQUENCY NIOBIUM CAVITY

M.C. Lin*, Ch. Wang, L.H. Chang, G.H. Luo, Synchrotron Radiation Research Center, Taiwan
F.S. Kao, M.K. Yeh, Department of PME, National Tsing Hua University, Taiwan
M.J. Huang, Department of ME, National Taiwan University, Taiwan

Abstract

A coupled-field analysis procedure is established to analyze the electromagnetic characteristics of a CESR-type 500 MHz SRF niobium cavity. The commercial code ANSYS is used as the solver and successfully links analyses of different fields. A shell structure for this shell-like cavity is modeled to analyze its mechanical behavior by finite element analysis, while a solid structure for the inner space is also modeled to analyze its high-frequency electromagnetic characteristics and resonant frequency. The shift of resonant frequency due to structure shrinkage when it is cooled down from 300K to 4.22 K is calculated. Some important parameters of this cavity, such as Epk/Eacc, Hpk/Eacc, and transit time factor are also calculated.

1 INTRODUCTION

A CESR-type 500 MHz superconducting cavity is going to be installed into the electron storage ring at SRRC, Taiwan [1, 2]. This cavity is made of bulk niobium sheet of 3 mm thickness. To operate it at low temperature, this cavity will be immersed in liquid helium with a good vacuum inside. Because this cavity is manufactured at room temperature, it shrinks when it is immersed into liquid helium. The resonant frequency and other characteristics at low temperature must be different from the ones at room temperature. To predict the RF characteristics at low temperature, a coupled-field model analysis is necessary. Conventionally two different numerical codes were used for computations of the electromagnetic field and structure deformation, separately. Thus the time-consuming work of model establishment has to be done at each analysis phase and errors are introduced in data transferring between models because the meshes can not be identical.

The commercial finite-element-analysis code ANSYS provides the ability to link the high-frequency (HF) analysis with thermal and structure analyses. Obviously this linked coupled-field analysis is more efficient because the model can be established by one single software and the related data can be transferred easily in between elements due to same mesh employed. It was applied to a calculation for PEP-II RF cavity to link with the RF loss and thermal distribution [2, 3], in which the 10-node tetrahedral elements HF119 and SOLID87 were used for electromagnetic and thermal calculations, respectively. Further work had been done [4] in which, by modeling with the commercial code MSC/PATRAN, the brick elements HF120, SOLID90, and SOLID95 were used for electromagnetic, thermal, and structure calculations, respectively, and successfully integrated in analyzing a Quasic-HOM free cavity.

In this work a similar analysis process is applied to the shell-type SC cavity. However, for better computational efficiency, the shell element SHELL93 is used to generate the bulk niobium cavity while the brick element HF120 for inner space. Also the commercial code MSC/PATRAN is used as the pre-processor to establish the geometry model and generate ANSYS-compatible mesh. All the meshes were established according to the cavity structure at room temperature. By applying material constants, temperature change, and pressure difference, the shell elements shrink to the shape at cold temperature. The RF characteristics of the cavity at cold can then be calculated by updating the coordinates of the shrunk shell surface.

2 CAVITY MODEL

Shown in Fig. 1 is the mesh of the CESR-type 500 MHz SC cavity. Because of symmetry, only 1/4 of the cavity was modeled while suitable boundary conditions were applied to the symmetry surfaces. Not only the cavity section, but also the round and flute beam tubes (RBT and FBT) are included in this model. However, the RF coupler and the cold waveguide are not included. A layer of shell element Shell93 covers the brick element HF120, and the nodes on the intersection are identical. There are 126170 nodes, 29472 HF120 elements, and 2422 SHELL93 elements in this model.

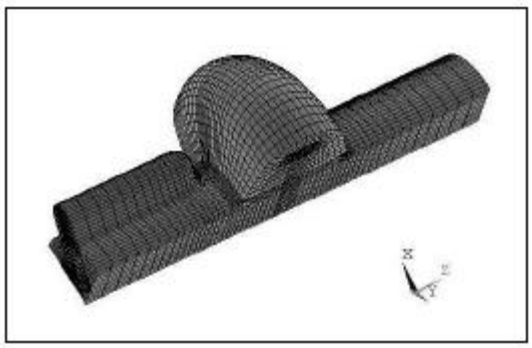

Figure 1: Finite element mesh of the CESR-type 500 MHz niobium cavity.

The element Shell93 must be established with all nodes at the middle plane of the shell structure, while the element HF120 must be assigned with boundary conditions at the outer surface. Here we care the RF characteristics more than the structure behavior, thus the

*chyuan@srrc.gov.tw

model is so constructed that the HF120 solid model matches the real cavity inner space while the Shell93 shell model is half thickness "shrunk" of the niobium sheet. Because the cavity is made of 3mm-thick niobium sheet and the inner radiuses of the equator and the round beam tube are 274 mm and 120 mm, respectively, this 1.5-mm shrunk is relatively small and the effects on the structure behavior are neglected.

At vertical test, the cavity is inserted into a helium vessel with the round beam tube downward. The helium vessel was filled with liquid helium so that the full cavity set is totally immersed. The liquid helium is saturated at 1 atm, thus the bath temperature is 4.22 K and the pressure is 101.330 kN/m^2. The inner vacuum is good than 1E-6 mbar and is negligible. These temperature and pressures are assigned to the FEM calculation as applied external loads.

The material constants used are
Young's modulus: 125 GPa [5]
Poisson's ratio: 0.38
integrated coefficient of thermal expansion: 4.94E-6 1/K.

3 CALCULATED RESULTS

3.1 Structure Deformation

As the cavity cooled from 300 K to 4.22 K, both the temperature change and the helium pressure shrink the cavity structure. Shown in Fig. 2 are the radial and longitudinal deformations, U_R and U_Z, on the edge of the cavity model. The location of cavity equator is shifted to Z=0 here. The nodes at the RBT end are fixed at longitudinal direction and the nodes at FBT end are constrained to have the same longitudinal displacement, thus Uz decreases from the FBT end to RBT end. The two small "jumps" happen at the cavity irises, the intersections of the cavity section and FBT and RBT. On the other hand, the radial displacement U_R has a more complicated behavior thanks to the FBT and cavity geometry. However, the negative U_R indicates the cavity section is smaller than the original shape and this predicts the resonant RF frequency will thus increase, which is proved by later HF analysis.

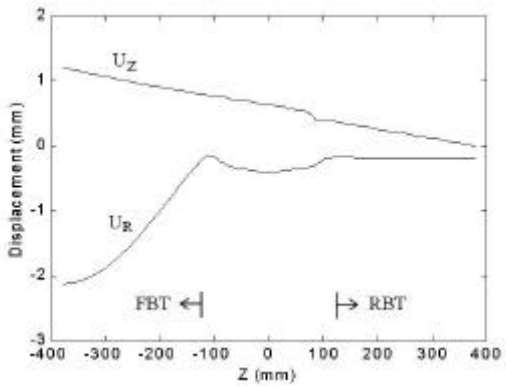

Figure 2: Radial and longitudinal displacements of the CESR-type 500 MHz cavity after cool down.

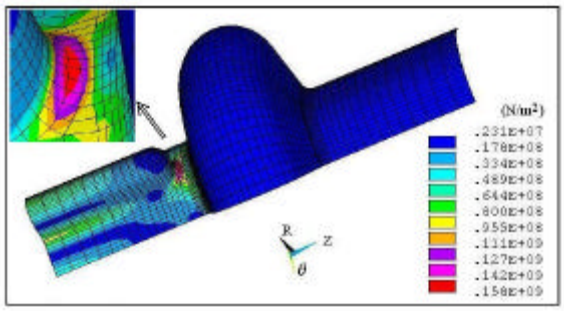

Figure 3: Equivalent stress on the CESR-type 500 MHz cavity after cool down.

The calculated equivalent stress σ_{eff} on the middle plane of each shell element is shown in Fig. 3. The equivalent stress σ_{eff} is calculated from the normal stresses σ_X, σ_Y, σ_Z and shear stresses τ_{XY}, τ_{YZ}, τ_{ZX} at each point as

$$s_{eff} = \frac{1}{2}\left(\left(s_X - s_Y\right)^2 + \left(s_Y - s_Z\right)^2 + \left(s_Z - s_X\right)^2 + 6\left(t_{XY}^2 + t_{YZ}^2 + t_{ZX}^2\right)\right)^{1/2} \quad (1)$$

The maximum σ_{eff}, 158 MPa, locates at the intersection tip of the flute convex and the beam tube, while the cavity section and the RBT have relatively small stress of less than 17.8 MPa everywhere. Note that the yielding stress of the niobium at 4 K is about 700 MPa [5].

3.2 RF Characteristics

The deformed cavity model was then used to compute the RF characteristics. In this study, only the TM_{010}-like mode is calculated. The most important RF characteristic is the accelerating electric field. Shown in Fig. 4 is the distribution of longitudinal electric field, E_Z, at accelerating voltage of 1.6 MV after cooling down.

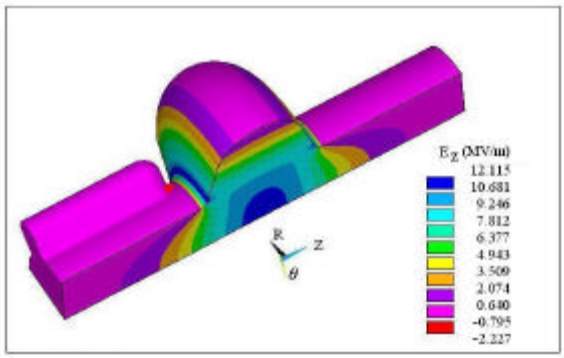

Figure 4: Distribution of longitudinal electric field of the CESR-type 500 MHz cavity after cool down at 1.6 MV accelerating voltage.

However, for the TM_{010}-like mode, the electric field is only longitudinal along the cavity axis, while it is normal

to the surface on the cavity wall. A comparison of these two distributions were shown in Fig. 5 with the on-axis accelerating voltage scaled to 1.6 MV, ie., average accelerating gradient E_{acc} of 5.33 MV/m. The peak electric field E_{pk} on axis is 11.42 MV/m and locates at the cavity center, while the peak normal electric field on surface is 13.27 MV/m and locates at the irises.

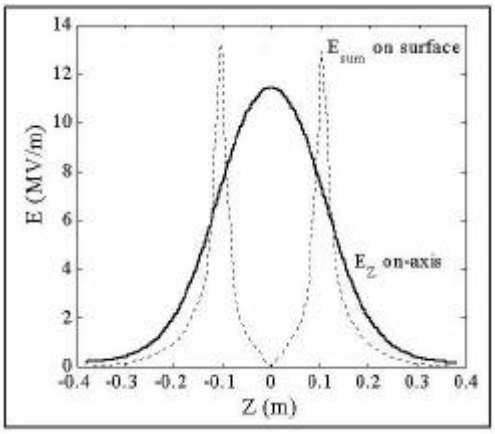

Figure 5: Longitudinal electric field on axis, E_Z, and normal electric field on the surface, E_{sum}, of the CESR-type 500 MHz cavity after cool down at 1.6 MV accelerating voltage.

Meanwhile, the surface magnetic field H is always parallel to the cavity wall. For TM_{010}-like mode, the surface magnetic field come from the circumferential magnetic field. Shown in Fig. 6 is the distribution of surface magnetic field at 1.6 MV accelerating voltage. The high magnetic field region locates around the equator, but the peak surface magnetic field H_{pk}, 22.437 kA/m, is not at the cavity equator anyway.

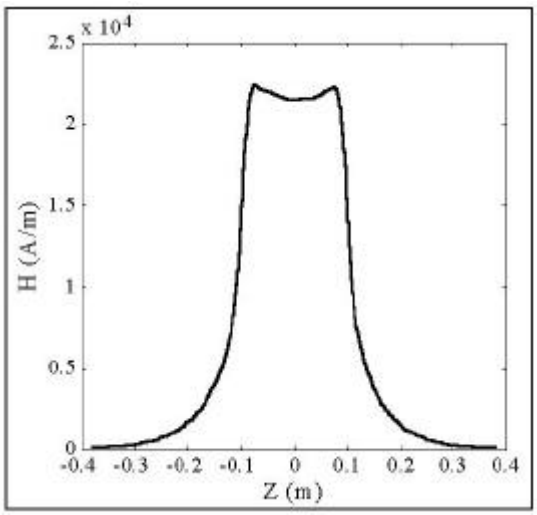

Figure 6: Surface magnetic field distribution of the CESR-type 500 MHz cavity after cool down at 1.6 MV accelerating voltage.

Listed in Table 1 are some important cavity parameters calculated. Both the results for cavity at warm and after cooling down are listed. For 300 K case, cavity vacuum was not considered. The resonant frequency shifts 668 kHz after cooling down. This prediction hints the cavity should be so tuned at warm to have a resonant frequency of some hundreds kHz lower than the desired operation frequency at cold. However, further studies are in progress to investigate the effects of liquid helium saturation pressure on the cavity RF characteristics.

Table 1 Calculated parameters of the CESR-Type 500 MHz cavity at warm and after cooling down

	300 K	4.222 K
Frequency (MHz)	500.636	501.304
Transit-time factor	0.504	0.505
E_{pk}/E_{acc} on-axis	2.14	2.14
E_{pk}/E_{acc} on surface	2.44	2.49
H_{pk}/E_{acc} on surface (kA/m/(MV/m))	4.19	4.21

4 CONCLUSIONS

By the coupled-field analysis process, the effects of cooling down on the superconducting cavity, especially the RF resonant frequency shift, can be predicted. Also the cavity structure deformation and stress distribution can be calculated. This is certainly a powerful analysis process on superconducting cavity design and characteristic prediction.

ACKNOWLEDGEMENT

This work is supported in part by National Science Council of Taiwan under Contract NSC-90-2213-E-213-001.

REFERENCES

[1] Ch. Wang, *et al.*, "Superconducting RF Project at the Synchrotron Radiation Research Center," 10th Workshop on RF Superconductivity, 2001.

[2] R. A. Rimmer *et al.*, "PEP-II RF Cavity Revisited," LBNL Report No. LBNL-45136, SLAC Report No. LCC-0032, 1999.

[3] R. A. Rimmer *et al.*, "RF Cavity R&D at LBNL for the NLC Damping Rings, FY1999," SLAC Report No. LCC-0033, 1999.

[4] M. C. Lin, et al., "A Coupled-Field Analysis on RF Cavity," PAC' 2001, pp. 1207-1209, 2001.

[5] M. G. Rao and P. Kneisel, "Mechanical Properties of High RRR Niobium," Advances in Cryogenic Engineering, Vol. 40, pp. 1383-1390, 1994.